2 OHKAWA, N.: 'Fiber-optic multigigabit GaAs MIC front-end circuit with inductor peaking', *ibid.*, 1988, **LT-6**, pp. 1665–1671
3 ENOKI, T., YAMASAKI, K., OSAFUNE, K., and OHWADA, K.: '0·3 μm advanced SAINT FETs having asymetric n^+-layer for ultra-high frequency GaAs MMICs', *IEEE Trans.*, 1988, **ED-35**, pp. 18–24
4 KAWANISHI, S., TAKADA, A., and SARUWATARI, M.: 'Wide-band frequency-response measurement of optical receivers using optical heterodyne detection', *J. Lightwave Technol.*, 1989, **LT-7**, pp. 92–98

DYNAMIC MODELLING OF DISTRIBUTED-FEEDBACK LASERS USING SCATTERING MATRICES

Indexing terms: Semiconductor lasers, Modelling, Transmission lines

A new technique for modelling DFB semiconductor lasers above threshold using scattering matrices is described. Quarter-wave-shifted grating devices are compared with unshifted devices under transient conditions.

Introduction: Distributed feedback (DFB) semiconductor lasers have a greater mode selectivity than Fabry–Perot devices, and so are preferred as sources for long-haul high-capacity fibre systems.[1] However, dynamic single-mode (DSM) operation is still difficult.[2] Accurate multimode dynamic computer models could help in designing DSM DFBs.

Many DFB models calculate the individual mode threshold gains in an attempt to assess wavelength stability.[3–5] However, these usually neglect the saturation and inhomogeneity of the gain which occurs at the onset of lasing.[6,7] Dynamic models are available, but these assume a single oscillating mode, making the study of mode stability impossible.[7]

This letter reports on a simple, numerically efficient, versatile technique to find DFB laser transient responses and spectra. This is based on scattering matrices solved in the time domain, and is a modification of the transmission-line laser model (TLLM).[8–11] The TLLM contrasts with transfer matrix models; these are solved in the frequency domain and are unsuitable for dynamic simulations or where saturation is present.[12,13]

Theory: The TLLM is based on a series of scattering matrices representing the optical processes which modify forward- and backward-travelling waves as they pass along the cavity.[8] These matrices are connected by transmission lines which represent the propagation delays of the waves and also serve to discretise time and space, allowing a digital computer to solve the network.

In Fabry–Perot TLLMs, the waves are only reflected at the facets. In DFB devices, the forward and backward waves are coupled along the entire cavity length because of a modulation of the guide dimensions. This coupling can be represented by impedance discontinuities placed between the model sections (Fig. 1).

The question is: how many model sections, each with a crosscoupling point, are required to represent this coupling accurately? A large number of sections, say two per grating period, would give a near-impossible computational task.[8]

Studies have shown that a very small number of cross-coupling points can mimic the wavelength response of a DFB

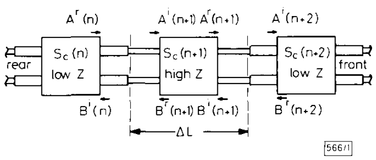

Fig. 1 *Three scattering matrices joined by transmission lines*

laser grating over a limited bandwidth. The condition was that the coupling per unit length κ must be the same as for the real device; i.e. the coupling per section must be increased to compensate for a small number of sections.

Two different matrices are required to represent the coupling: one for a high-low impedance transition (section n to section $n+1$, where n is an odd integer); and one for a low-high impedance transition (section $n+1$ to section $n+2$). These can be derived by assuming that the admittances of the lines are modulated by $\pm\Delta Y$ from their mean admittance Y. For small modulations, ΔY can be related to the coupling per unit length κ using[14]

$$\Delta Y/Y = \kappa\Delta L \tag{1}$$

where ΔL is the mean length of the model sections and equal to half the model's grating period Λ. This ensures that stopband lies at the centre of the modelled bandwidth.

The matrix describing the low-high impedance transition and the transmission lines connecting the main scattering matrices, was derived from standard transmission-line equations, giving

$$_{k+1}\begin{bmatrix} A(n+1) \\ B(n) \end{bmatrix}^i = \begin{bmatrix} 1+\kappa\Delta L & -\kappa\Delta L \\ \kappa\Delta L & 1-\kappa\Delta L \end{bmatrix} {}_k\begin{bmatrix} A(n) \\ B(n+1) \end{bmatrix}^r \tag{2}$$

For a high-low impedance transition the matrix becomes

$$_{k+1}\begin{bmatrix} A(n+2) \\ B(n+1) \end{bmatrix}^i = \begin{bmatrix} 1-\kappa\Delta L & \kappa\Delta L \\ -\kappa\Delta L & 1+\kappa\Delta L \end{bmatrix} {}_k\begin{bmatrix} A(n+1) \\ B(n+2) \end{bmatrix}^r \tag{3}$$

where k is the iteration number and i denotes incident pulses to the main scattering matrices $\boldsymbol{S}_c$, and r denotes reflected pulses from the main scattering matrices. Note that there is a one iteration time-step delay as the optical field samples move along the lines.

For a standard DFB device,[1] eqns. 2 and 3 are applied alternately along the device length, i.e. $n = (1, 3, 5, 7 \ldots)$. For quarter-wave-shifted grating devices,[4] a zero-reflection interface (identify matrix) is inserted half-way along the cavity.

Results: The dynamic and spectral properties of standard and quarter-wave-shifted 1550 nm DFBs have been compared. The device parameters were taken from References 1 and 15. The devices were subject to an injection current step to 100 mA, resulting in a transient overshoot. 98 model sections were used and κL was 3·2.

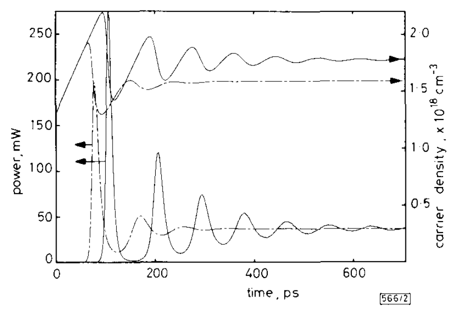

Fig. 2 *Transient responses and average carrier concentrations of unshifted (solid) and quarter-wave-shifted (broken) DFB lasers*

Fig. 2 shows the power transients of the two devices. Note that the shifted device had a shorter turn-on delay, a greater damping of the transient and a higher relaxation oscillation frequency. The threshold carrier density was also lower in the shifted device, as expected.[4] The steady-state output powers were similar, indicating near-equal quantum efficiencies.

Fourier transforms revealed the devices' spectra (Fig. 3). The unshifted device had two modes separated by 3·9 nm, as previously observed.[1] The mode powers were random because of spontaneous emission. The sidelobes correspond to the

10 GHz resonance of the output powers. The shifted device had a single mode at the centre of the stopband. Making the gain peak wavelength carrier dependent would show non-random mode partition effects.[15]

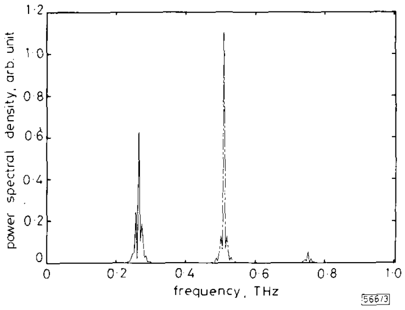

Fig. 3 *Spectra of two lasers during first 230 ps*

Conclusions: A simple modification to the TLLM allowed the dynamics of DFB lasers to be studied. The model could be easily extended to DBR structures, DFB amplifiers and DFBs with external feedback. Future work will concentrate on including laser chirp effects,[11] allowing the study of frequency-modulatable multisection devices.

Acknowledgment: I thank G. Motosugi of NTT, Japan for interesting discussions and the initial inspiration during ECOC'88.

A. J. LOWERY 26th July 1989

Department of Electrical & Electronic Engineering
University of Nottingham
University Park, Nottingham NG7 2RD, United Kingdom

References

1 WESTBROOK, L. D., HENNING, I. D., NELSON, A. W., and FIDDYMENT, P. J.: 'Spectral properties of strongly coupled 1·5 μm DFB laser diodes', *IEEE J. Quantum Electron.*, 1985, **QE-21**, pp. 512–518

2 SASAKI, S., CHOY, M. M., and CHEUNG, N. K.: 'Effects of dynamic spectral behaviour and mode-partitioning of 1550 nm distributed feedback lasers on Gbit/s transmission systems', *Electron. Lett.*, 1988, **24**, pp. 26–28

3 HENRY, C. H.: 'Performance of distributed feedback lasers designed to favor the energy gap mode', *IEEE J. Quantum Electron.*, 1985, **QE-21**, pp. 1913–1918

4 MCCALL, S. L., and PLATZMAN, P. M.: 'An optimised $\pi/2$ distributed feedback laser', *ibid.*, 1985, **QE-21**, pp. 1899–1904

5 TROMBERG, B., OLESEN, H., PAN, X., and SAITO, S.: 'Transmission-line description of optical feedback and injection locking for Fabry–Perot and DFB lasers', *ibid.*, 1987, **QE-23**, pp. 1875–1889

6 DULING, I. N., and RAYMER, M. G.: Time-dependent semiclassical theory of gain-coupled distributed feedback lasers', *ibid.*, 1984, **QE-20**, pp. 1202–1207

7 KINOSHITA, J.-I., and MATSUMOTO, K.: 'Transient chirping in distributed feedback lasers: effect of spatial hole-burning along the laser axis', *ibid.*, 1988, **QE-24**, pp. 2160–2169

8 LOWERY, A. J.: 'New dynamic semiconductor laser model based on the transmission line modelling method', *IEE Proc. J., Optoelectron.*, 1987, **134**, pp. 281–290

9 LOWERY, A. J.: 'A new time-domain model for spontaneous emission in semiconductor lasers and its use in predicting their transient response', *Int. J. Numer. Modell.*, 1988, **1**, pp. 153–164

10 LOWERY, A. J.: 'Transmission-line modelling of semiconductor lasers: the transmission-line laser model', submitted to *Int. J. Numer. Modell.*, July 1989

11 LOWERY, A. J.: 'Model for multimode picosecond dynamic laser chirp based on transmission line laser model', *IEE Proc. J., Optoelectron.*, 1988, **135**, pp. 126–132

12 BJORK, G., and NILSSON, O.: 'A new exact and efficient numerical matrix theory of complicated laser structures: properties of asymmetric phase-shifted DFB lasers', *J. Lightwave Technol.*, 1987, **LT-5**, pp. 140–146

13 MAKINO, T., and GLINSKI, J.: 'Transfer matrix analysis of the amplified spontaneous emission of DFB semiconductor laser amplifiers', *IEEE J. Quantum Electron.*, 1988, **QE-24**, pp. 1507–1518

14 THOMPSON, G. H. B.: 'Physics of semiconductor laser devices' (Wiley, NY, 1980), Chap. 8

15 WESTERBROOK, L. D.: 'Measurements of dg/dN and dn/dN and their dependence on photon energy in 1·5 μm InGaAsP laser diodes', *IEE Proc. J, Optoelectron.*, 1986, **133**, pp. 135–142

MULTICHANNEL Ku-BAND OSCILLATOR WITH DIELECTRIC RESONATORS

Indexing terms: Microwave devices and components, Microwave oscillators, Dielectrics, Resonators

The theory, design and realisation of a multichannel Ku-band oscillator with eight dielectric resonators (DRs) are described. Selection of a single DR is achieved by *pin* diodes. The oscillator stability, phase noise and signal level are comparable with available high-quality DROs. Stability is better than 3 ppm/°C, phase noise is 85–90 dBc/Hz at 10 kHz, and the signal level is 16–18 dBm. The device is compact, simple and cheap.

Introduction: For fixed-frequency signal generation it is normal to use oscillators with dielectric resonators (DROs), for their simplicity, small dimensions and weight, low power consumption and low price. However, for systems with many radio channels as well as for devices with frequency-hopping, it is necessary to use more DROs with multiplex switches to achieve channel selection. This is achieved using a multichannel DRO which consists of an amplifier, *n* DRs and *n pin* diodes.

Theory: The multichannel DRO block diagram is shown in Fig. 1. One of the eight DRs is activated by the corresponding *pin* diode switch within the amplifier feedback circuit. The *pin* diode polarisation is provided by chokes. The phase of the signal in each feedback line is approximately the same, to provide constant working conditions for the amplifier. It must be ensured that the inactive lines do not influence the line which forms the feedback loop.

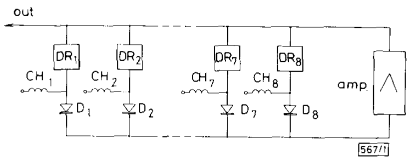

Fig. 1 *Block diagram of multichannel DRO with eight DRs*

In the analysis of the oscillating conditions, the DR was described by an equivalent circuit, shown in Fig. 2. The *S*-parameters of the equivalent circuit were calculated using Reference 1. The touchstone program was used for the design of the feedback circuit.

In the example presented here, a frequency range from 14 to 14·5 GHz is covered using eight DRs and eight *pin* diodes.

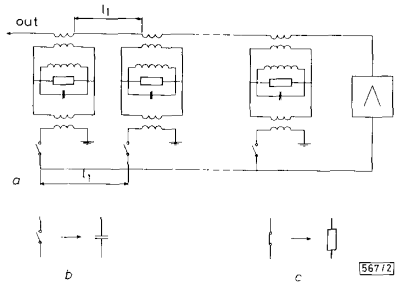

Fig. 2 *Multichannel DRO simulated with equivalent circuit*